Drifting solitary waves in a reaction-diffusion medium with differential advection

Arik Yochelis[1] and Moshe Sheintuch[1]

[1]*Department of Chemical Engineering, Technion – Israel Institute of Technology, Haifa 32000, Israel*

(Received May 15, 2009)

Propagation of solitary waves in the presence of autocatalysis, diffusion, and symmetry breaking (differential) advection, is being studied. The focus is on drifting (propagating with advection) pulses that form via a convective instability at lower reaction rates of the autocatalytic activator, i.e. the advective flow overcomes the fast excitation and induces a drifting fluid type behavior. Using spatial dynamics analysis of a minimal case model, we present the properties and the organization of such pulses. The insights underly a general understanding of localized transport in simple reaction-diffusion-advection models and thus provide a background to potential chemical and biological applications.

PACS numbers: 47.35.Fg, 82.40.Ck, 47.20.Ky, 47.54.-r

arXiv:0905.2629v1 [nlin.PS] 15 May 2009

Solitary waves are prominent generic solutions to reaction-diffusion (RD) systems and basic to many applied science disciplines [1]. In one spatial dimension, these spatially localized propagating pulses are qualitatively described by a fast excitation (leading front) from a rest state followed by a slow recovery (rear front) to the same uniform state [1]. Thus, in isotropic RD media a single symmetric supra-threshold localized perturbation results in *counter-propagating* pulses or wave trains [2].

However, in chemical and biological media transport can be facilitated by both diffusion and advection and thus excitation properties of solitary waves can be subjected to convective instabilities [3]. Nevertheless, theoretical foundations of solitary waves in the presence of a symmetry breaking advective transport, i.e. dynamics in a differential reaction-diffusion-advection (RDA) media, are yet to be established. Among a few reported examples, it was only shown both experimentally and numerically (with no underlying theoretical basis), that excitable pulses can persist in RDA with a propagation direction against the advective field [4], i.e. upstream.

In this Letter we analyze an RDA case model and demonstrate that under low reaction rates, solitary waves may become convectively unstable and thus *drift* (see Fig. 1), i.e. the slow recovery becomes a leading front. We reveal the regions and the properties of such drifting pulses and show that the phenomenon underlies a competition between a local kinetics of the activator and a differential advection. Our methods include a bifurcation theory of coexisting spatial solutions (linear analysis and numerical continuations) coupled to temporal stability; all the results well agree with direct numerical integrations. At the end, we discuss the potential applicability of our findings to chemical and biological media.

Model setup.– We start with a minimal RDA model that incorporates local kinetics of activator $v(x,t)$ and inhibitor $u(x,t)$ type:

$$\begin{aligned} u_t + s u_x &= f(u,v) - u, \\ Le\, v_t + s v_x &= B f(u,v) - \alpha v + Pe^{-1} v_{xx}. \end{aligned} \tag{1}$$

These dimensionless equations describe a membrane (or cross-flow) reactor, with continuous feeding and cooling in which an exothermic reaction takes place $f(u,v) \equiv Da(1-u)\exp\left[\gamma v/(\gamma+v)\right]$ [6]. Eq. (1) admits a uniform rest state $(u,v) = (u_0, v_0 \equiv Bu_0/\alpha)$, where u_0 obtained via $Da = u_0(1-u_0)^{-1}\exp\left[-\gamma u_0/(\gamma\alpha/B+u_0)\right]$. In what follows, we set $Pe = 15$, $s = 1$, $\alpha = 4$, $\gamma = 10000$, and use Le, Da and B as control parameters allowed to vary; parameter definitions are given in [7].

A standard linear stability analysis to periodic perturbations, shows that the uniform states (u_0, v_0) may loose stability to two finite wavenumber Hopf instabilities, $Da^{\pm}$, that emerge from (B^W, Da^W), as shown in Fig. 1; the instabilities are of a drifting type, i.e. in direction of advection. This anomaly arises due to the broken reflection symmetry of left-right traveling waves that is preserved in RD systems. We note that traveling waves TW^- bifurcate (nonlinearly) subcritically from Da^- while traveling waves TW^+ bifurcate supercritically from Da^+ [5]. While the region $Da^- < Da < Da^+$ is linearly unstable, under certain conditions stationary periodic (SP) solutions may also develop. The criterion for SP states is zero of the real and the imaginary parts in the dispersion relation (for a finite wavenumber), identifying zero speed [5] (see dotted line in Fig. 1).

Here, our interest is in the affect of a differential advection (Le) and the local kinetics (B, Da) on the organization of drifting solitary waves. We also consider large domains in which pulse behavior is not affected by the type of boundary conditions (periodic, no-flux or mixed) and also not interested in the regimes in which nonuniform steady state patterns may form, for details on the affect of boundary conditions see [5].

Propagation of solitary waves.– To reveal the propagation properties and the regimes of solitary waves (see Fig. 1), we look at the steady state version of (1) in a comoving frame, $\xi = x - ct$ [5]:

$$\begin{aligned} u_\xi &= (s-c)^{-1}\left[Daf(u,v) - u\right], \quad v_\xi = w, \\ w_\xi &= Pe\left[(s - cLe)\, w - BDaf(u,v) + \alpha v\right]. \end{aligned} \tag{2}$$

The advantage is that existence of nonuniform states can be now analyzed via spatial dynamics methods, i.e. where space is viewed as a time-like variable. Thus, solitary waves [in the context of (1)] become in (2) asymmetric homoclinic orbits

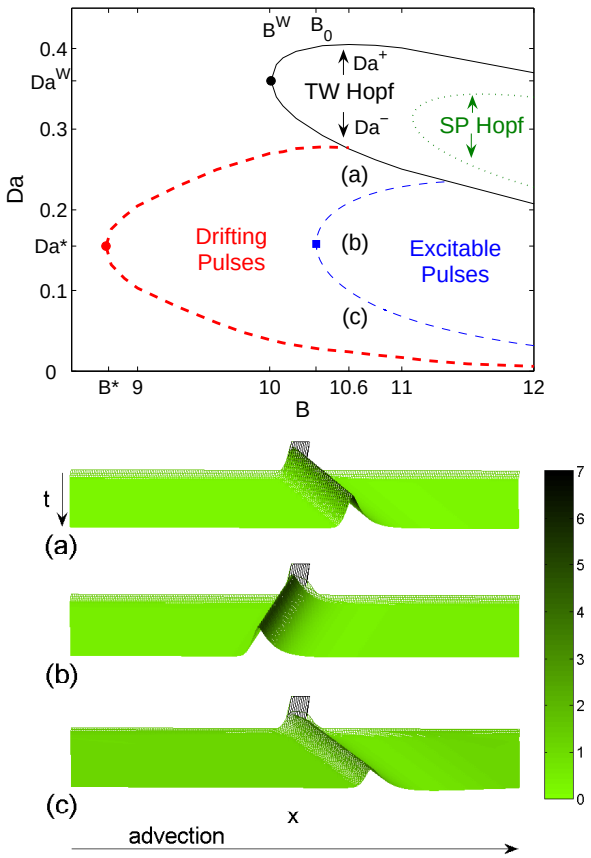

FIG. 1: (color online) Top panel: Regions of excitable (thick dashed line) and drifting (thin dashed line) solitary waves (pulses) in a reaction rate parameter space (B, Da) at $Le = 100$; the thin dashed line implies zero velocity of a pulse. The solid line mark the onsets of finite wavenumber instabilities of traveling waves, $TW^{\pm}$. The dotted line marks the criterion for stationary periodic (SP) solutions (see text for details). The (●), marks the leftmost limits of homoclinic orbits $(B^*, Da^*) \simeq (8.76, 0.155)$ and asymmetric finite wavenumber Hopf bifurcation $(B^W, Da^W) \simeq (10, 0.36)$ while (■) marks the leftmost limit of excitable pulses $(B_0, Da^*) \simeq (10.35, 0.155)$. Bottom panel: Space-time plots at $B = 10.6$ and (a) $Da = 0.24$, (b) $Da = 0.15$, and (c) $Da = 0.08$. The plots show $v(x,t)$ resulting from integration of Eq. (1) with no-flux boundary conditions, where $x \in [0, 10]$ and $t \in [0, 2265]$; we used a top-hat initial condition embedded in (u_0, v_0) at the respective Da values.

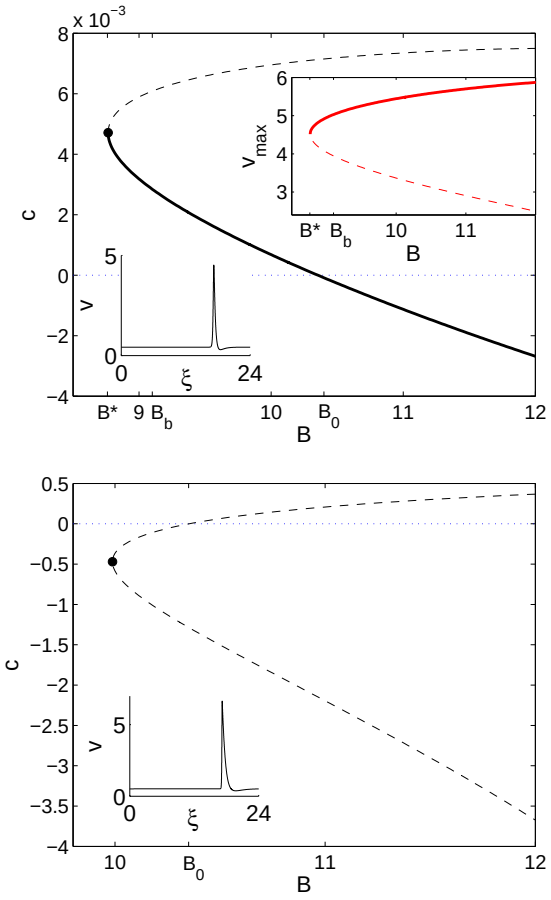

FIG. 2: (color online) Bifurcation diagrams showing the branches of homoclinic solutions as a function of B at $Da^* \simeq 0.155$ and $Le = 100$ (top panel) and $Le = 1$ (bottom panel). The branches are plotted in terms of the propagation speed and the maximal value of $v(\xi)$ (top inset); solid lines indicate linear stability. Bottom insets show profiles of $v(\xi)$ at the two folds, marked by (●). The branches were obtained via integration of Eq. (2) while the stable portions of each branch coincide with solutions obtained by integration of Eq. (1); here the periodic domain is $L = 24$ but results are identical also on larger domains.

(HO) and $TW^{\pm}$ (which will be also discussed) correspond to periodic orbits undergoing Hopf bifurcations at $Da^{\pm}$ (with a proper c). In the following all these solutions will be computed numerically using a continuation package AUTO [8], where the speed c is obtained as a nonlinear eigenvalue problem. Then temporal stability of such steady states will be calculated employing an eigenvalue problem via Eq. (1) in a comoving frame.

In Fig. 2(top panel), we present the branches of HO at $Da = Da^* \simeq 0.155$ (a horizontal cut in top panel in Fig. 1), resulting via a simultaneous variation of (B, c). $B = B^* \simeq 8.76$ identifies a fold, where the stable branch corresponds to large amplitude HO (see inset). The drifting pulses exist for $B^* < B < B_0 \simeq 10.35$ since both branches have positive speeds, and have similar profiles (see inset) as the standard excitable pulses. Namely, drifting pulses propagate in the direction of the advection (downstream, $c > 0$) where the leading front is the oscillatory tail that was a trailing tail above $B = B_0$, for excitable pulses (upstream, $c < 0$).

Drifting pulses are expected at low reaction rate regimes of the activator, represented in (1) by dimensionless rate constant (Da) and exothermicity (B). Under such conditions the excitation of nearest neighbors is suppressed due to the advective flow (a nonlinear convective instability) and thus the pulse after speed reversal is no longer excitable since the leading front now develops from the rest state as a small amplitude perturbation. This scenario changes once the differential advection is eliminated ($Le = 1$), in this case a typical RD behavior is

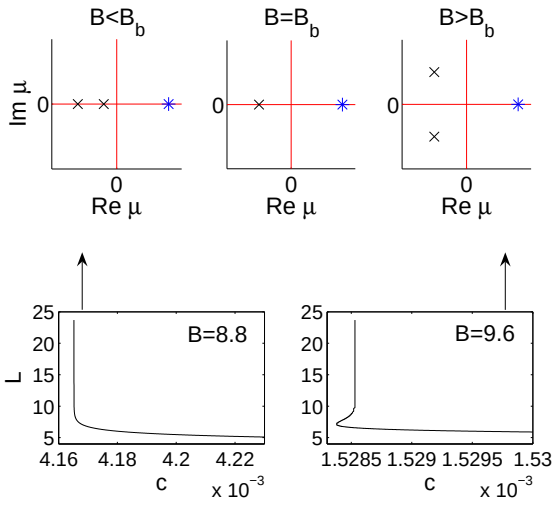

FIG. 3: (color online) Top panel: Schematic representation of typical eigenvalue configurations about the uniform state $(u_0, v_0, 0)$ corresponding to a saddle if $B < B_b$ and a saddle-focus if $B > B_b$, where $B_b \simeq 9.1$ is the Belyakov point. Bottom panel: Typical dispersion relations that associated with the respective eigenvalues computed starting from the stable homoclinic orbits (see top panel). Parameters as in the top panel of Fig 2.

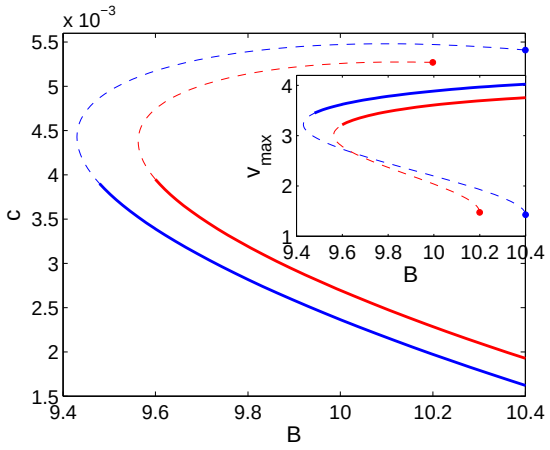

FIG. 4: (color online) Bifurcation diagram showing the branches of traveling waves (TW^-) as a function of B in terms of speed and the maximal value of $v(\xi)$ (in the inset), at $B = 10.4$ (dark line) and $B = 10.2$, where $Da^- \simeq 0.29, k_c \simeq 3.2, c \simeq 0.0054$ and $Da^- \simeq 0.31, k_c \simeq 3.355, c \simeq 0.0053$, respectively. Solid lines imply linear stability to long wave lengths perturbations [9], while (●) marks the respective onsets of the linear finite wavenumber Hopf bifurcation to TW^-. Integration details as in the top panel of Fig. 2 but on distinct periodic domains.

restored. While the $c = 0$ line for $Le = 1$, in the (B, Da) plane doesn't change, we show in Fig. 2(bottom panel) that near the fold only a negative velocity region forms, i.e. a standard excitable pulses are being restored (stability of the pulses does not play a qualitative role).

Nevertheless, drifting pulses in presence of a differential advection inherit the properties of excitable pulses, as demonstrated by monotonic and nonmonotonic dispersion relations in Fig. 3. The latter are important characteristics of organization and interaction of solitary waves [10] and are distinguished here around $B = B_b \simeq 9.1$, a so called Belyakov point [11]. At this point and with an appropriate speed, the spatial eigenvalues [of Eq. (2)] correspond to one positive real (associated with $\xi \to -\infty$) and a degenerate pair of negative reals (associated with $\xi \to \infty$). Below B_b, the degeneracy is removed but the eigenvalues remain negative reals (a saddle) while above B_b they become complex conjugated corresponding to a saddle-focus (a Shil'nikov type HO [12]), marked by $(\times)$ in top panel of Fig. 3. Importantly, such an interchange of eigenvalues implies a transition from monotonic to oscillatory dispersion relation [Fig. 3(bottom panel)] and a monotonic (in space) approach of the HO to the fixed point as $\xi \to \pm\infty$, which implies coexistence of bounded-pulse states for $B > B_b$ [10].

Organization of drifting states.– A standard theory of solitary waves qualitatively predicts an organization of HO to be accompanied by periodic solutions [12]. Here the dispersion relations obtained at $B < B^W$ [Fig. 3(bottom panel)], indeed imply existence of periodic orbits although the uniform state is linearly stable. These periodic solutions are in fact TW^- that bifurcate subcritically from the locus of points $Da = Da^-$ for $B > B^W$ [with distinct critical wavenumbers and speeds obtained from the linear analysis of Eq. (1)], as shown by two examples in Fig. 4. Notably, there are infinite number of such TW^- families. Unlike the HO, stability of TW^- solutions do depend on domain size [9].

The organization of all drifting nonuniform solutions can be understood by varying Da at two representative B values. Fig. 5(a), shows a bifurcation diagram of nonuniform solutions at $B \simeq 10.4$: while $TW^\pm$ propagate downstream. The single pulse HO branch ends at the two rightmost ends (marked by dots), at which the profiles take the form of homoclinic tails (see bottom inset) [13]. Due to the proximity to the subcritical onset of TW^- at Da^-, the two rightmost ends ever approach each other as domain (L) is increased, and consequently, they inherit the propagation direction of the top and the bottom branches of TW^- as discussed in [5]. As B is decreased below B^W the HO and the TW^- solutions organize in isolas and parts of their stability regions overlap [Fig. 5(b)], implying sensitivity to initial perturbations. Note that the oscillations of the right tail in the profile had decreased (see bottom inset), which is consistent with the approach towards Belyakov point $(B = B_b)$.

Conclusions and prospects.– We have showed that solitary waves can propagate bidirectionally (without changing their shape) due to a competition between activator autocatalysis and a symmetry breaking advection. Consequently, we distinguish between excitable (upstream or against advection) and drifting (downstream or with advection) propagations. The former is a characteristic behavior of RD systems and persists while the reaction rate of the activator is dominant (analogues

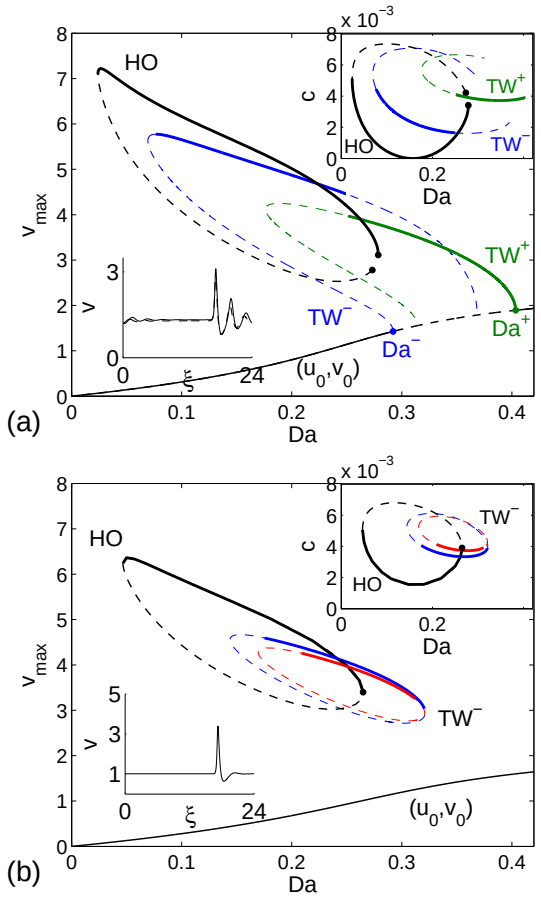

FIG. 5: (color online) Bifurcation diagram showing the branches of uniform states (u_0, v_0), homoclinic orbits (HO), and traveling waves $(TW^{\pm})$ as a function of Da in terms of the maximal value of $v(\xi)$ at (a) $B = 10.4$ and (b) $B = 9.6$. Solid lines imply linear stability, including stability of $TW^{\pm}$ to long wave lengths perturbations [9], while $Da^{\pm}$ mark the onsets of the linear finite wavenumber Hopf bifurcation to $TW^{\pm}$, respectively. The top inset represents the nonuniform states in terms of speed while the large (small) isola corresponds to the TW^{-} family emerging from Da^{-} at $B = 10.4$ ($B = 10.2$). The bottom shows HO profiles at locations marked by (●); in (a) the two dots mark also the two ends of the HO branch. Integration details as in the top panel of Fig. 2 but on distinct periodic domains.

to front dynamics [14]). While the latter is a consequence of low excitation and thus subjected to a nonlinear convective instability resulting in a fluid type behavior. Through a bifurcation analysis of spatial extended steady states arising in a minimal RDA model, we revealed the properties and the organization of drifting pulses. Since the results center on homoclinic orbits which known to act as organizing centers of spatial solutions, qualitative applicability to systems with other autocatalytic properties is naturally anticipated.

Up-to-date only excitable (upstream) solitary waves have been observed experimentally in an autocatalytic RDA system [4], nevertheless chemical media operated in cross-flow (membrane) tubular reactors [6] or on a rotating disks [15], are the most natural setups to confirm our predictions and explore technological directions. Moreover, theoretical insights explored here can be related to a profound puzzle of large intracellular particles (organelles) self-organization, in eucaryotic cells [16]. For example, localized aggregations of myosin-X within the filopodia have been observed to propagate bidirectionally [17] and from the modeling point of view argued to be driven by both diffusion and differential advection [18]. Consequently, a theoretical framework integrating autocatalytic kinetics and distinct transport, is paramount to promoting a mechanistic understanding of spatiotemporal trafficking of intracellular molecular aggregations.

We thank to N. Gov and M. Naoz for the helpful discussion on molecular motors. This work was supported by the US-Israel Binational Science Foundation (BSF) and A.Y. was also partially supported by the Center for Absorption in Science, Israeli Ministry of Immigrant Absorbtion. M.S. is a member of the Minerva Center of Nonlinear Dynamics and Complex Systems.

[1] E. Meron, Phys. Rep. **218**, 1 (1992); M.C. Cross and P.C. Hohenberg, Rev. Mod. Phys. **65**, 851 (1993).
[2] A. Yochelis, E. Knobloch, Y. Xie, Z. Qu, and A. Garfinkel, Europhys. Lett. **83**, 64005 (2008).
[3] J.M. Chomaz, Phys. Rev. Lett. **69**, 1931 (1992).
[4] M. Kærn and M. Menzinger, Phys. Rev. E **65**, 046202 (2002).
[5] A. Yochelis and M. Sheintuch, e-print: arXiv:nlin.PS/0810.4690; e-print: arXiv:nlin.PS/0902.2688.
[6] O. Nekhamkina, B.Y. Rubinstein, and M. Sheintuch, AIChE J. **46**, 1632 (2000).
[7] Le (Lewis number), is the ratio of solid- to fluid-phase heat capacities, Pe (Péclet number), is the ratio of convective to conductive enthalpy fluxes, and Da (Damköhler number), is the dimensionless rate constant [6].
[8] E. Doedel *et al.*, *AUTO2000: Continuation and bifurcation software for ordinary differential equations (with HOMCONT)*, http://indy.cs.concordia.ca/auto/.
[9] Temporal stability of $TW^{\pm}$ was computed for large periodic domains, $L = n\lambda_c, n > 1, \lambda_c \equiv 2\pi/k_c$ (until the onset didn't change with n), via a standard numerical eigenvalue method using Eq. (1) in a comoving frame. k_c is the critical wavenumber at the Hopf onset.
[10] C. Elphick, E. Meron, J. Rinzel, and E.A. Spiegel, J. Theor. Biol. **146**, 249 (1990); M. Or-Guil, I.G. Kevrekidis, and M. Bär, Physica D **135**, 154 (2000).
[11] L.A. Belyakov, Mat. Zametki **28**, 910 (1980).
[12] P. Glendinning and C.T. Sparrow, J. Stat. Phys. **35**, 645 (1984); N.J. Balmforth, Annu. Rev. Fluid Mech. 27, 335 (1995); A.R. Champneys *et al.*, SIAM J. Appl. Dyn. Syst. **6**, 663 (2007).
[13] J. Sneyd, A. LeBeaub, and D. Yule, Physica D **145**, 158 (2000).
[14] V. Yakhnin and M. Menzinger, Chem. Eng. Sci. **57**, 4559 (2002); M. Sheintuch, Y. Smagina, and O. Nekhamkina, Ind. Eng. Chem. Res. **41**, 2136 (2002).
[15] Y. Khazan and L.M. Pismen, Phys. Rev. Lett. **75**, 4318 (1995).
[16] M.A. Welte, Curr. Biol. **14**, R525 (2004).
[17] J.S. Berg and R.E. Cheney, Nature Cell. Biol. **4**, 246 (2002).
[18] D.A. Smith and R.M. Simmons, Biophys. J. **80**, 45 (2001).